Published in final edited form as:
J Tissue Eng Regen Med. 2014 January ; 8(1): 15–28. doi:10.1002/term.1487.

Effect of Grafting BMP2 Derived Peptide to Nanoparticles on Osteogenic and Vasculogenic Expression of Stromal Cells

Angel E. Mercado[1], **Xiaoming Yang**[2], **Xuezhong He**[1], and **Esmaiel Jabbari**[1]

[1]Biomimetic Materials and Tissue Engineering Laboratory, Department of Chemical Engineering, University of South Carolina, Columbia, SC 29208, USA

[2]Dorn Research Institute, Columbia, SC 29209, USA

Abstract

Bone morphogenetic protein-2 (BMP2) plays a major role in initiating the cascade of osteogenesis. However, high doses of exogenous BMP2 coupled with diffusion away from the intended site cause adverse side effects. An alternative is to use biodegradable polymeric nanoparticles (NPs) grafted with peptides of the active domains of BMP2. NPs present a multivalent form of the peptide for stronger interaction with cell surface receptors, leading to a stronger activation of osteogenic signaling pathways. The objective of this work was to compare osteogenic activity of the BMP2 peptide (BMP2Pe), corresponding to residues 73–92 of BMP2 protein (BMP2Pr), grafted to biodegradable NPs with that of BMP2 protein (BMP2Pr). BMP2Pe was functionalized with a cysteine residue and grafted to poly(lactide fumarate) and poly(lactide-co-ethylene oxide fumarate) (PLAF/PLEOF) NPs via a thioether link. The calcium content of bone marrow stromal (BMS) cells cultured in osteogenic media supplemented with BMP2 peptide/protein grafted NPs (BMP2Pe-gNP and BMP2Pr-gNP) was slightly higher than other BMP2 treated groups, but all osteogenic groups showed similar levels of mineralization after 21 days. The expression pattern of master transcription factors Dlx5 and Runx2 indicated that BMP2 protein induced a faster osteogenic signaling than the BMP peptide. The expression level of Osteopontin, Osteocalcin, and PECAM-1 in the NP grafted BMP2 groups was significantly higher than those of ungrafted BMP2Pr and BMP2Pe groups, which may be due to a more effective presentation of the peptide/protein to cell surface receptors, thus leading to a stronger interaction of the peptide/protein with clustered cell surface receptors.

Keywords

nanoparticles; grafting; bone morphogenetic peptide; osteogenesis; marrow stromal cells; gene expression

Corresponding author: Esmaiel Jabbari, Ph.D. Associate Professor of Chemical and Biomedical Engineering Swearingen Engineering Center, Rm 2C11 University of South Carolina Columbia, SC 29208 Tel: (803) 777-8022 Fax: (803) 777-0973 jabbari@engr.sc.edu.

Financial disclosure Authors have no conflict of interest or financial interest from this work to disclose.

1. Introduction

Osteogenic differentiation factors play a central role in modulation and control of cell migration, maturation, and morphogenesis (Lisi et al., 2003). In particular, recombinant human bone morphogenetic protein-2 (BMP2), used clinically in spine fusion, plays a major role in initiating the cascade of chemotaxis, differentiation of bone marrow stromal (BMS) cells and bone regeneration (Ripamonti *et al*., 1997; Wozney, 2002). BMP2 induces bone formation *in vivo* in ectopic and orthotopic sites (Yasko et al., 1992; Yamagiwa et al., 2001). Since BMP2 signaling is highly regulated *in vivo* (Hillger et al., 2005; Lin et al., 2008), much higher doses (1 mg/mL) than the endogenous amount have to be loaded in the graft to induce bone formation (McKay *et al*., 2002). However, high doses coupled with the diffusion of BMP2 away from the intended site of regeneration (Lee *et al*., 2007) cause adverse effects such as bone overgrowth, immunological reaction, and tumorigenesis (Kleeff *et al*., 1999; Langenfeld *et al*., 2003; Shields *et al*., 2006). In an effort to reduce protein diffusion and increase residence time, encapsulation in nano/micro particles or grafting to a carrier is used to immobilize BMP2 in the site of regeneration (Liu *et al*., 2006; Chen *et al*., 2007; Chung *et al*., 2007; Wei *et al*., 2007; Fu *et al*., 2008; Lin *et al*., 2008). For example, BMP2 conjugated to a porous collagen-coated poly(lactide-co-glycolide) (PLGA) scaffold reduced free lateral diffusion and internalization of BMP2/receptor complex, leading to enhanced differentiation of osteoprogenitor cells and bone formation (Liu *et al*., 2006). BMP2-conjugated PLGA nanoparticles in a fibrin gel enhanced bone formation in a critical size rat calvarial defect (Chung *et al*., 2007). BMP2 immobilized on a heparin-conjugated fibrin gel showed a higher extent of bone formation compared to direct addition of the protein to the gel (Yang et al., 2010). Those results may be attributed to the interaction of the protein with heparin, leading to a prolonged residence time of BMP2 in the regeneration site. In another study, Chen and collaborators showed BMP2 encapsulated in dextran-glycidylmethacrylate/poly(ethylene glycol) microspheres induced higher expressions of alkaline phosphatase and osteopontin in human periodontal ligament cells (Chen et al., 2006). BMS cells displayed higher expression of osteopontin and osteocalcin after 7–12 days of incubation in osteogenic media supplemented with BMP2 grafted biodegradable nanoparticles (NPs), compared to the direct addition of BMP2 to the culture media (Mercado *et al*., 2009).

Those results demonstrate that encapsulating BMP2 in NPs can prolong the residence time of the protein in the regeneration site. In addition, BMP2 grafting to NPs can provide a much higher localized concentration of the protein at the cell surface, leading potentially to a more intense activation of osteogenic pathways and expression of osteogenic markers. However, the very high doses of BMP2 loaded in the graft, as free protein or attached to NPs, can cause tumor formation in some patients (Shields *et al*., 2006). BMP2 not only is a potent inducer of osteogenic differentiation, it also plays a major role in cell migration and angiogenesis. BMP2 can promote vascularization and is involved in tumor angiogenesis by stimulating the activation of transcription factor inhibitor of differentiation-1 (Id1) and phosphorylation of p38 mitogen-activated protein kinase (Langenfeld *et al*., 2004; Raida *et al*., 2005). It has been shown that BMP2 promotes motility of smooth muscle cells by activation of Wnt pathways (Perez et al., 2011).

An attractive alternative to reduce the undesired side effects of BMP2 is to use peptides to induce osteogenesis of progenitor cells. Peptides based on the active domains of BMP2 are two orders magnitude less costly to produce than the protein and they are much less likely to induce tumor formation because their biological function is significantly limited compared to the protein (Gabet et al., 2004; Saito et al., 2004; Behnam et al., 2005). For example, the peptide LYLTSIASLETPVSSAKPIK (hereafter designated as BMP2Pe), corresponding to residues 73–92 of the knuckle epitope of BMP2, promotes mineralization when implanted in a rat tibial bone defect (Saito *et al*., 2003; Saito *et al*., 2004). Furthermore, BMP2Pe has a significantly higher alkaline phosphatase (ALPase) activity than sequences 68–87, 68–92, 78–97, and 44–58 and inhibits BMP2 from binding to both type I and type II BMP receptors (Saito *et al*., 2003). However due to their smaller size and higher diffusivity, peptides need to be immobilized by grafting to NPs for presentation to cell surface receptors and to reduce their diffusion away from the site of regeneration. We hypothesized that BMP2Pe grafted to resorbable NPs would provide a multivalent form of the peptide for a stronger interaction with cell surface receptors to induce a higher expression of osteogenic markers, thus leading to accelerated bone repair and reduced side effects.

Our laboratory has developed novel poly(lactide fumarate) (PLAF) and poly(lactide-co-ethylene oxide fumarate) (PLEOF) macromers that self-assemble to form NPs (He et al., 2008). In the process of NP formation, the PLEOF macromer acts as a stabilizer to produce NPs ranging 50–500 nm in size. The lactide and glycolide units of the NPs are FDA approved for certain clinical applications, ethylene oxide units are excreted through the kidneys, and fumaric acid units occur naturally in the Kreb's cycle. Peptides and proteins can be attached by a thioether or succinimide link to the NPs. The objective of this study was to synthesize BMP2 peptide grafted PLAF/PLEOF NPs and compare its osteogenic activity with that of BMP2 protein grafted NPs in marrow stromal cell cultures.

2. Materials and methods

2.1. Materials

L-lactide (LA; >99.5% purity) monomers were obtained from Ortec (Easley, SC) and Boehringer Chemicals (Ingelheim, Germany), respectively. LA monomers were dried under vacuum at 40°C for at least 12 h. Calcium hydride, ninhydrin reagent, tetrahydrofuran (THF), deuterated chloroform (99.8% deuterated), trimethylsilane (TMS), Poly(ethylene glycol) (PEG, nominal molecular weight 3.4 kDa), triethylamine (TEA), tin (II) 2-ethylhexanoate (TOC), and dimethylsulfoxide (DMSO) and piperidine were purchased from Aldrich (Sigma-Aldrich, St. Louis, MO). PEG was dried by azeotropic distillation from toluene. Fumaryl chloride (FC) was obtained from Aldrich and distilled at 161°C prior to use. Diethylene glycol (DEG; >99% purity) was purchased from Fisher (Pittsburgh, PA). The protected amino acids and Rink Amide NovaGel resin were purchased from EMD Biosciences (San Diego, CA). *N*,*N*-Dimethylformamide (DMF), methylene chloride (DCM), *N*,*N*′-diisopropylcarbodiimide (DIC), triisopropylsilane (TIPS), *N*,*N*-dimethylaminopyridine (DMAP), hydroxybenzotriazole (HOBt) and trifluoroacetic acid (TFA) were received from Acros Organics (Pittsburgh, PA). Diethyl ether and hexane were obtained from VWR (Bristol, CT). DCM was dried by distillation over calcium hydride. Spectro/Por dialysis tube

(molecular weight cutoff 3.5 kDa) was purchased from Spectrum Laboratories (Rancho Dominquez, CA). N,N'-disuccinimidyl carbonate (DSC) was obtained from Novabiochem (EMD Biosciences, San Diego, CA). Ethylenediaminetetraacetic acid disodium salt (EDTA), penicillin, streptomycin, Alizarin red, and paraformaldehyde were purchased from Sigma (St. Louis, MO). Dulbecco's phosphate-buffered saline (PBS) and Dulbecco's Modified Eagle's Medium (DMEM; 4.5 g/L glucose with L-glutamine and without sodium pyruvate) were obtained from GIBCO BRL (Grand Island, NY). Trypsin and fetal bovine serum (FBS, screened for compatibility with rat BMS cells) were obtained from Invitrogen (Carlsbad, CA) and Atlas Biologicals (Fort Collins, CO), respectively. Quant-it PicoGreen dsDNA reagent kit was obtained from Invitrogen (Carlsbad, CA). QuantiChrom calcium and alkaline phosphatase assay kits were purchased from Bioassay Systems (Hayward, CA). BMP2 solution (100 μL, 1.5 mg/mL in BMP2 buffer) was generously donated by Medtronic (Minneapolis, MN). Antibodies (Anti-Tubulin (sc-5286), anti-RUNX2 (sc-10758) and anti-DLX5 (sc-18152)) were from Santa Cruz Biotechnology (Santa Cruz, CA).

2.2. Macromer Synthesis

Low molecular weight poly(L-lactide) (LMW-PLA) was synthesized by ring-opening polymerization of LA (100%) monomers as previously described (He *et al*., 2008; Jabbari *et al*., 2009). Next, PLAF macromer was synthesized by condensation polymerization of LMW-PLA with FC as described (He *et al*., 2008). Similarly, PLEOF was synthesized by condensation polymerization of LMW-PLA and PEG with FC as described (He *et al*., 2007). Succinimide-terminated PLAF-NHS macromers were produced by reacting the hydroxyl end-groups of PLAF macromers with DSC, as described (Mercado *et al*., 2009). Briefly, 800 mg PLAF and 26 mg DSC were mixed in 15 mL DMF in a reaction flask. After purging with nitrogen, 40 μL TEA was added while stirring, and the reaction was allowed to continue for 8 h at ambient conditions. The chemical structure of the macromers was characterized by a Varian Mercury-300 ^{1}H-NMR (Palo Alto, CA) as described (He *et al*., 2008). The number-average ($\overline{m_n}$), weight-average ($\overline{m_w}$), and polydispersity index (PDI) of the macromers were measured with a Waters 717 Plus Autosampler GPC system (Waters, Milford, MA) connected to a styragel HT guard column (7.8 mm×300 mm) in series with a styragel HR 4E column (7.8 mm×300 mm) as described (He *et al*., 2008). The $\overline{m_n}$, $\overline{m_w}$, and PDI of the LMW-PLA were 1450 Da, 1730 Da, and 1.2. The $\overline{m_n}$, $\overline{m_w}$, and PDI of the synthesized PLAF were 4.5 kDa, 8.61 kDa, and 1.9, respectively; and 4.7 kDa, 8.63 kDa and 1.83 for PLAF-NHS.

2.3. Nanoparticle self-assembly

Mixtures of PLAF (or PLAF-NHS) and PLEOF macromers were self-assembled into NPs by dialysis, as shown in Figure 1. Briefly, a mixture of 45 mg PLAF (or PLAF-NHS) and 5 mg PLEOF dissolved in 1 ml dimethylformamide (DMF) and 8 ml dimethylsulfoxide (DMSO) was loaded in a dialysis tube and dialyzed against sterile PBS for 24 h with change of PBS buffer every 2–4 h (Mercado *et al*., 2009). After self-assembly, the NPs suspension was freeze-dried to obtain a free flowing powder. The shape and morphology of the NPs were examined using a JSM-5400 scanning electron microscope (JOEL, Japan) at an accelerating voltage of 20 KeV (He *et al*., 2008). Prior to SEM imaging, freeze-dried NPs were coated with gold using an Ion Sputter Coater (JEOL, JFC-1100) at 20 mA for 1 min.

The NPs size distribution was measured by dynamic light scattering with a NICOMP Submicron Particle Sizer (Autodilute Model 370, NICOMP Particle Sizing Systems, Santa Barbara, CA) (He *et al*., 2008). The scattered light intensity was inverted to size distribution by inverse Laplace transform using the CW370 software (NICOMP Particle Sizing Systems). The zeta potential of the NPs was measured in HEPES buffer (200 μg/mL NPs) by a ZetaPlus analyzer (Brookhaven Instruments, Holtsville, NY) as described (Xie *et al*., 2005). To determine mass loss with time, 50 mg NPs were suspended in 1 ml PBS and the suspensions were incubated at 37°C until complete degradation (no mass remaining or NPs not detectable by dynamic light scattering) (Mercado *et al*., 2008). At each time point, samples were freeze-dried and mass of the dried powder was measured. The fraction of mass remaining was determined by dividing the dried mass at time t by the initial mass at time zero.

2.4. Peptide synthesis and grafting

The cysteine-terminated BMP2 derived peptide C-KIPKA SSVPT ELSAI STLYL (BMP2Pe) was synthesized on Rink Amide NovaGel resin in the solid phase using a previously described procedure (He et al., 2008) and functionalized by the addition of a cysteine residue at the N-terminal. Briefly, the Fmoc-protected amino acid (6 equiv), DIC (6.6 equiv), and HOBt (12 equiv) were added to 100 mg resin and swelled in DMF. Next, 0.2 mL of 0.05 M DMAP was added to the mixture and the coupling reaction was allowed to proceed for 4–6 h at 30°C with orbital shaking. The resin was tested for the presence of unreacted amines using the Kaiser reagent (Kaiser et al., 1970). If the test was positive, the coupling reaction was repeated. Otherwise, the resin was treated with 20% piperidine in DMF and the next Fmoc-protected amino acid was coupled using the same procedure. The BMP2Pe was cleaved from the resin by treating with 95% TFA/2.5% TIPS/2.5% water and precipitated in cold ether. For grafting, 2 mL of the NPs suspension (10 mg NPs) was centrifuged at 15,000 rpm for 10 min, the supernatant was decanted, and the NPs were re-suspended in 0.5 mL PBS by sonication for 1 min with an ultrasonic processor (3-mm probe, Cole-Parmer, Vernon Hills, IL). Next, 0.5 mL BMP2Pe (20 mg/mL with PLAF NPs) or BMP2Pr (400 ng/ mL with PLAF-NHS NPs) solution was added to the NPs suspension and the grafting reaction was allowed to continue overnight at ambient conditions (see Figure 1). The grafting reaction for the peptide produced a thioether link between the cysteine residue on the peptide and the fumarate group on the NPs, while the succinimide group of the PLAF-NHS NPs reacted with free amine groups of the BMP2Pr. The suspension was centrifuged at 15000 rpm for 10 min and the amount of ungrafted peptide and protein in the supernatant was quantified by the ninhydrin reagent as described (Kaiser *et al*., 1970). For analysis, 200 μl of the supernatant was incubated at 37°C for 12 h and 50 μl of ninhydrin reagent was added. After mixing, the sample was heated to 120°C for 5 min and the absorbance was measured at 570 nm with a Synergy HT plate reader (Synergy HT, BioTek, Winooski, VT). The measured absorbance was related to concentration using a calibration curve constructed from the absorbance of solutions with known concentrations of BMP2Pe and BMP2Pr. Conjugation efficiency was determined by dividing the amount of attached (total minus free) peptide or protein by the total amount.

For determination of BMP2 peptide or BMP2 protein release kinetics, 10 mg grafted NPs was incubated with 1 ml PBS at 37°C with orbital shaking. At each time interval, the suspension was centrifuged at 15000 rpm for 10 min, and the amount of peptide or protein in the supernatant was measured. The amount of BMP2 peptide was measured with the ninhydrin reagent as described above (Kaiser *et al*., 1970). The amount of enzymatically active BMP2 protein was measured by ELISA using the BMP Quantikine kit as described (Mercado *et al*., 2008). The fraction of released peptide or protein was determined by dividing the measured amount at each time point to the total grafted amount at time zero.

2.5. Bone marrow stromal cell isolation and culture

BMS cells were isolated from the bone marrow of young adult male Wistar rats according to established protocols (He *et al*., 2008; He *et al*., 2010). Cell isolations were performed under a protocol approved by the Institutional Animal Care and Use Committee of the University of South Carolina. After aseptically removing femurs and tibias, the marrow was flushed out with 20 mL of cell isolation media (DMEM supplemented with 100 units/mL penicillin (PEN), 100 μg/mL streptomycin (SP), 20 μg/mL fungizone (FZ) and 50 μg/mL gentamicin sulfate (GS)). The cell suspensions were centrifuged at 200×g for 5 min, cell pellets were re-suspended in 12 mL basal media (DMEM supplemented with 10% FBS, 100 units/mL PEN, 100 μg/mL SP, 50 μg/mL GS and 250 ng/mL FZ) and aliquoted into T-75 flasks. The flasks were subsequently maintained in a humidified 5% CO_2 incubator at 37°C. Cultures were washed with PBS and replaced with fresh media at 3 and 7 days to remove haematopoietic and other unattached cells. After 10 days, cells were detached from the flasks with 0.05% trypsin-0.53 mM EDTA and used for *in vitro* experiments.

2.6. Osteogenic activity of BMP2Pe grafted NPs

BMS cells were seeded in 24-well plates at a density of 5×10^4 cells/mL in basal medium. After 24 h for cell attachment (time zero), the medium was replaced with standard osteogenic medium (basal media supplemented with 100 nM dexamethasone (DEX), 50 μg/mL ascorbic acid (AA), 10 mM β-glycerophosphate (βGP)) supplemented with protein and peptide grafted NPs (equivalent to 200 ng of the grafted enzymatically-active BMP2Pr or BMP2Pe) and incubated for the indicated period of time. At each time point for analysis (4, 7, 11, 14, and 18 days), the culture medium was collected, centrifuged at 15000 rpm, supernatant was removed, and the precipitate was resuspended in fresh osteogenic medium and added to the seeded cells. The cultured cells after removing the medium at each time point were washed with PBS, lysed (10mM Tris, 2% triton), centrifuged, and the supernatant was used for determination of DNA and calcium contents, immunostaining, and mRNA analysis. BMP2 and BMP2Pe (200 ng/mL) directly added to the BMS cell cultures at time zero in osteogenic medium were used as the positive controls (Vehof et al., 2001). BMS cells cultured in osteogenic medium (OM) and OM supplemented with blank PLAF NPs were used as negative controls.

2.7. Measurement of DNA content, ALPase activity and calcium concentration

The double stranded DNA (dsDNA) content of the samples was measured using a Quant-it PicoGreen assay according to the manufacturer's instructions. An aliquot (100μL) of

working solution was added to 100μL of the cell lysate and incubated for 4 min at ambient conditions. The solution fluorescence was measured with a Synergy HT plate reader at emission and excitation wavelength of 485 and 528 nm, respectively (Mercado *et al*., 2008). Measured intensities were correlated to cell numbers using a calibration curve constructed with BMS cells of known concentration ranging from zero to 4×10^4 cells/mL. ALPase activity was assessed using QuantiChrom ALPase Assay Kit according to manufacturer's instructions. A 10 μL aliquot of the sonicated cell lysate was added to 190 μL of the reagent solution containing 10 mM pnitrophenyl phosphate and 5mM magnesium acetate and absorbance was recorded at time zero and again after 4 min. ALPase activity was calculated using the equation $[(A_{t=4}\text{-}A_{t=0})/(\text{Acalibrator-}A_{ddH2O})\times808]$ expressed as IU/L. The absorbance was measured on a Synergy HT microplate reader at 405 nm. The measured ALPase activity was normalized to the DNA content. Calcium content was measured using QuantiChrom calcium assay kit according to the manufacturer's instructions. 0.2 mL of 2M HCl was added to 0.2 mL aliquot of the sonicated cell lysate to dissolve the calcium content of the mineralized matrix (Mercado *et al*., 2009). Next, 5 μL aliquot of the supernatant was added to 200μL of the working solution of the kit. After incubation for 3 min, the absorbance was measured on a plate reader at 612 nm. Measured intensities were correlated to equivalent amounts of Ca^{2+} using a calibration curve constructed with $CaCl_2$ solutions of known concentration ranging from zero to 200 μg/mL.

2.8. Cell morphology and immunostaining

At each time point (7 and 21 days), samples were washed with PBS and fixed in 4% paraformaldehyde at ambient conditions for 1 h. They were then permeabilized with 0.1% Triton X-100 and 100 mM glycine in PBS for 30 minutes and blocked in 1.5% bovine serum albumin (BSA), 0.5 mM glycine in PBS for 1 hour at ambient conditions. Next, samples were incubated with the primary antibody in PBS containing 1% BSA (1:50 to 1:200 dilution) for 24 h at 4°C according to manufacturer's instructions. Primary antibodies from Santa Cruz Biotechnology (Santa Cruz, CA) included mouse anti-rat OP, rabbit anti-rat OC, and goat anti-rat PECAM-1. After washing with PBS, samples were incubated with the secondary antibody (1:100 dilution) in blocking buffer for 1 h at ambient conditions. Secondary antibodies from Santa Cruz Biotechnology included donkey anti-mouse FITC-conjugated IgG, donkey anti-rabbit Texas-red conjugated IgG, and donkey anti-goat Texas-red conjugated IgG. For morphological studies, samples were incubated with 0.16 μM Alexa Fluor® 594 phalloidin (Invitrogen, Carlsbad, CA) and 300 nM DAPI (4,6-diamidino-2-phenylindole; Sigma) for 30 min at ambient conditions to stain the cell actin filaments and nuclei, respectively. Samples were imaged with a Nikon Eclipse Ti-ε inverted fluorescent microscope. Secondary antibodies without the primaries were used as negative controls.

2.9. NPs interaction with cells

For imaging, the NPs were loaded with 2 wt% Fluorescein isothiocyanate (FITC, Sigma-Aldrich, excitation and emission wavelength of 450/495 and 520 nm). Next, the seeded BMS cells were incubated in standard osteogenic media supplemented with 2 mg/mL FITC-loaded NPs for up to 24 h. At each time point the suspension was removed, cells were washed three times with PBS to remove the unattached NPs, and processed and stained with phalloidin and DAPI as described above. Samples were imaged with an inverted fluorescent

microscope (Nikon Eclipse Ti-ε, Nikon, Melville, NY). At each time point, the fluorescent intensity of the attached NPs was quantified with a Synergy HT plate reader at 520 nm. Measured intensities were correlated to equivalent amounts of NP using a calibration curve constructed with suspensions of known FITC-loaded NP concentration.

2.10. mRNA Analysis

At each time point, total cellular RNA was isolated using TRIzol (Invitrogen, Carlsbad, CA) or RNeasy Mini-Kit (Qiagen, Valencia, CA) according to the manufacturer's instructions. The qualitative and quantitative analysis of the RNA samples was performed with NanoDrop 2000 (Thermo Scientific, Waltham, MA). The obtained RNA histograms and gel images were analyzed for the intact 28S and 18S ribosomal RNA. 1μg of the extracted total RNA was subjected to cDNA conversion using the Reverse Transcription System (Promega, Madison, WI). The obtained cDNA was subjected to real time polymerase chain reaction (PCR) amplification with appropriate gene specific primers. The expression levels of ribosomal protein S16 were used as the endogenous control. Primers for real-time PCR analysis were designed and selected using the Primer3 web-based software as described (Henderson *et al*., 2008; Jabbari *et al*., 2009). The PCR products were analyzed by agarose gel electrophoresis with 2% ethidium bromide staining (Sigma). The annealing temperatures and other parameters for amplification were optimized by classical PCR and agarose gel electrophoresis as described (Henderson *et al*., 2008; Jabbari *et al*., 2009). Real-time PCR (RT-qPCR) was performed to analyze the differential expression of OP, OC, PECAM-1, Runx2 and Dlx5 genes with SYBR green RealMasterMix (Eppendorf, Hamburg, Germany) using Bio-Rad CXF96 machine (Bio-Rad, Hercules, CA). The following forward and reverse primers were synthesized by Integrated DNA technologies (Coralville, IA): Osteopontin: forward 5′-GAC GGC CGA GGT GAT AGC TT-3′ and reverse 5′-CAT GGC TGG TCT TCC CGT TGC-3′; Osteocalcin: forward 5'-AAA GCC CAG CGA CTC T-3′ and reverse 5'-CTA AAC GGT GGT GCC ATA GAT-3′; PECAM-1: forward: 5′-CGA AAT CTA GGC CTC AGC AC-3′ and reverse: 5′-CTT TTT GTC CAC GGT CAC CT-3′; *Dlx5*: forward 5′- CCT CAT GGC TAC TGC TCT CC-3′ and reverse 5′-CTC GGC CAC TTC TTT CTC TG-3′; *Runx2*: forward 5′-GCC GGG AAT GAT GAG AAC TA-3′ and reverse 5′-GGA CCG TCC ACT GTC ACT TT-3′; S16: forward 5′-AGT CTT CGG ACG CAA GAA AA-3′ and reverse 5′-AGC CAC CAG AGC TTT TGA GA-3′ (Henderson *et al*., 2008; Ciarmela *et al*., 2009). Quantification of gene expression was based on the crossing-point threshold value (CT; number of cycles required for the RT-qPCR fluorescent signal to cross the threshold) for each sample. This was evaluated by the Relative Expression Software Tool (RESTTM) (Pfaffl, 2001) as the average of three replicate measurements. The model of Pfaffl, which includes an RT-qPCR efficiency correction factor of the individual transcripts, was used to determine the expression ratio of the gene (Pfaffl, 2001). The expression of S16 housekeeping gene was used as the reference and the fold difference in gene expression was normalized to the first time point.

2.11. Statistical analysis

Data are expressed as means±standard deviation. All experiments were done in triplicate. Significant differences between groups were evaluated using a two-tailed Student's t-test. A value of $p<0.05$ was considered statistically significant.

3. Results

3.1. Characterization of PLAF and PLAF-NHS NPs

The NPs had spherical shape, as imaged by SEM, and a normal distribution. The average size and breadth of the PLAF and PLAF-NHS NPs was 240±80 nm and 242±70 nm, respectively. The grafting efficiency was 70±5% for BMP2Pe to PLAF NPs and 97±0.5% for BMP2Pr to PLAF-NHS NPs. The average size and breadth of the BMP2Pe grafted NPs (BMP2Pe-gNP) and BMP2Pr grafted NPs (BMP2Pr-gNP) was 250±90 nm and 260±80 nm, respectively. There was no statistically significant difference between the size of BMP2Pe and BMP2Pr grafted NPs. The zeta potential of the NPs (with or without grafting) was negative which was attributed to the ionized carboxylic acid chain-ends of PLAF and PLEOF. The zeta potential of PLAF NPs was −55±2 mV, which was close to the reported value of −45 mV for PLGA NPs (Sahoo et al., 2002). The zeta potential of BMP2Pe-gNP and BMP2Pr-gNP increased slightly to −45±3 and −47±3 mV compared to ungrafted NPs, consistent with previous results. For example, the zeta potential of PLGA NPs became less negative after coating with amphiphilic polymers like poloxamer-407 and poloxamine-908 (Redhead et al., 2001). In another study, the zeta potential of polystyrene (with carboxylic end groups) NPs increased from −49 to −44 mV after coating with albumin (Foster et al., 2001). Overall, there was no statistically significant difference between the zeta potential of the ungrafted, BMP2Pe grafted, and BMP2Pr grafted NPs.

The release kinetic of BMP2 peptide and BMP2 protein from the NPs is shown in Figure 3b. It should be noted that Figure 3b shows the fraction of BMP2 protein released in enzymatically active conformation, as measured by ELISA, while the profile for BMP2 peptide is the fraction of total grafted peptide. We have previously shown that incubation time does not affect stability of BMP2 protein (Mercado *et al*., 2009). The release profiles followed the degradation kinetics of the NPs shown in Figure 3c. Mass loss was nearly linear in the first four weeks of incubation in which 80% of the mass loss occurred. Nearly 45% of the active BMP2 protein and all of BMP2 peptide were released in the first four weeks of incubation.

3.2. NPs interaction with cells

To determine the extent of interaction and uptake of NPs, FITC encapsulated NPs were incubated with BMS cells. The images of the FITC-loaded NPs (green FITC) without grafting, with BMP2 peptide grafting, and with BMP2 protein grafting in contact with BMS cells (blue nuclei and red cytoskeleton) after 24 h of incubation in osteogenic media are shown in Figures 2a, 2b, and 2c, respectively. The fraction of NPs attached to the BMS cells with or without BMP2 peptide/protein grafting is shown in Figure 3a with incubation time. The uptake fraction increased with incubation time for all NPs with or without grafting. The uptake fraction was slightly higher for peptide/protein grafted NPs compared to ungrafted NPs but the difference was statistically significant only for the 6 h time point (shown by a star in Figure 3a).

3.3. Cell morphology

Morphology of the BMS cells after 7 and 21 days of incubation in different culture conditions is shown in Figure 4. Experimental groups included BMS cells cultured in basal medium (A), osteogenic medium (OM, B), OM supplemented with 200 ng/mL BMP2Pe (C), OM supplemented with 200 ng/mL BMP2Pe grafted NPs (D), OM supplemented with 200 ng/mL BMP2Pr (E), and OM supplemented with 200 ng/mL BMP2Pr grafted NPs (F). The fluorescent images on the left and right correspond to 7 and 21 days, respectively. Cells in all groups exhibited the typical spindle-shape polygonal morphology of BMS cells (Mauney et al., 2004; Nadri et al., 2007). BMS cells cultured in basal medium (images A7 and A21) did not show a change in morphology from 7 to 21 days, while those cultured in osteogenic medium (images B–F) exhibited clustering and aggregation, suggesting BMS cells underwent differentiation in osteogenic medium. BMS cells cultured in OM supplemented with BMP2Pe grafted NPs, BMP2Pr, and BMP2Pr grafted NPs showed the highest extent of aggregation, forming star and circular patterns (Fig 4 D21, E21, F21).

3.4. Expression of genes in BMP signaling pathway

Dlx5 and Runx2 are critical transcription factors in the BMP signaling, and are required for osteogenesis (Lee et al., 2003; Lee et al., 2003; Hassan et al., 2006). To assess whether BMP2Pe or BMP2Pr grafted NPs enhanced the expression of Dlx5 and Runx2, their expressions are compared at the mRNA level in Figure 5. The BMP2 protein groups (grafted and free) induced high expression of both *Dlx5* and *Runx2* mRNA at 4 and 7 days, but their expressions decreased to baseline levels at day 21. Cells that were exposed to BMP2Pe (grafted and free) did not have an increased expression of *Dlx5* and *Runx2* at early time points (day 4 and 7) compared to the cells incubated in OM with or without blank NPs. However, BMP2Pe significantly enhanced the expression of Dlx5 and Runx2 at day 14 and 21. These results suggested that unlike BMP2 protein that acutely induced osteogenic differentiation of BMS cells, the effect of BMP2 peptide was delayed.

3.5. Expression of osteogenic and vasculogenic markers

Osteopontin (OP) and Osteocalcin (OC) are the markers of osteogenesis and PECAM is the marker of vasculogenesis. The expression levels of OP, OC and PECAM are shown in Figure 6. The expression of OP in BMP2 protein treated cells was higher at the early time point (day 4). OP expression in BMP2Pe-gNP and BMP2Pr-gNP groups was significantly higher than the control (OM) at all time points (indicated by one star in Figure 6). More importantly, BMP2Pr or BMP2Pe conjugated to the NPs induced a significantly higher expression of OP than free BMP2Pr and BMP2Pe during day 7–21 (indicated by two and three stars, respectively). For OC, its expression level in BMP2Pr-gNP group was significantly higher than all other osteogenic groups at day 7 and 14. The expressions of OC in BMP2Pe-NP and BMP2Pr-gNP groups were much higher than other groups at 21 days. For PECAM, its expression levels in BMP2Pe-gNP and BMP2Pr-gNP groups were much higher than other osteogenic groups at late time points (day 14 and 21), while its expression did not differ dramatically among these groups during early time points. Overall, the expression of OP, OC, and PECAM in BMP2Pe-gNP and BMP2Pr-gNP groups was significantly higher than those in the other osteogenic groups after 21 days, suggesting that

BMP2 conjugated to NPs had a sustained effect on inducing osteogenesis and vasculogenesis. In the osteogenic groups, OP was activated prior to the up-regulation of OC, consistent with OP and OC being the early and late markers of osteogenesis, respectively (Aubin et al., 1995). The increase in OP, OC, and PECAM expressions in osteogenic groups supplemented with BMP2 was consistent with the findings of Hu and collaborators (Hu et al., 2005). They observed significantly higher mRNA expressions of OP, OC, and VEGF when BMS cells were treated with BMP2. The higher PECAM expression in OM cultures supplemented with BMP2 was consistent with the reported enhancement in neovascularization and stimulation of blood vessel formation in tumors by BMP2 (Langenfeld *et al.*, 2004).

The expression of OP and OC (osteogenic markers) and PECAM (vasculogenic marker) in BMS cells are shown in the left (green), center (yellow), and right (red) images of Figure 7, respectively. BMS cells cultured in basal medium showed a weak expression of OP and OC, and no expression of PECAM (A images in Figure 7). BMS cells cultured in OM medium showed a relatively intense expression of OP, a weak expression of OC, and no expression of PECAM (B images). However, BMS cells cultured in OM supplemented with BMP2Pe-gNP (D images), BMP2Pr (E images), and BMP2Pr-gNP (F images) showed relatively intense expression of all three markers. In particular, BMS cells cultured in OM supplemented with BMP2Pe-gNP and BMP2Pr-gNP showed the highest expression of PECAM compared to the other groups (see images D-PECAM and F-PECAM). These results suggests that BMP2 (peptide or protein) grafted to the NPs enhance induction of BMS cell differentiation.

3.6. DNA content, ALPase activity, and Calcium concentration

DNA contents of the six groups are shown in Figure 8. A relatively high seeding density (5×10^4 cells/cm^2) was used because cell-cell contact plays a critical role in the differentiation of adherent BMS cells (Huss et al., 1995). At day 4, DNA content of the cells cultured in OM was higher than those cultured with BMP2Pr and BMP2Pe and followed a similar trend in day 21. The DNA content of BMP2Pe-gNP and BMP2Pr-gNPs was similar to that of OM at day 4 but decreased significantly to the level of BMP2Pr and BMP2Pe groups after 21 days as the cells underwent osteogenic differentiation. From day 7, the DNA content of all BMP groups (grafted or not) was statistically lower than that of OM (indicated by a star in Figure 8). For example, DNA content of BMP2Pe-gNP changed from 567±34 to 494±9, 458±19 and 414±26 ng/mL after 4, 7, 14, and 21 days, respectively, while that of BMP2Pr-gNP changed from 579±8 to 473±10, 446±5 and 415±11 ng/mL. This trend was consistent with previous reports that cell number decreases with differentiation of BMS cells in osteogenic medium supplemented with BMP2 (Owen et al., 1990; Shi et al., 2010).

ALPase activity and calcium content of the BMS cells in the six groups are shown in Figure 8. ALPase activity of all BMP groups (with and without grafting) significantly increased (indicated by one star with respect to OM) from day 4 to 7, remained at an elevated level at day 14, and then returned to the baseline level after 21 days. This was consistent with our previous results (He *et al.*, 2008) that the peak ALPase activity indicates the start of mineralization. Calcium content of all groups increased significantly with incubation from 4

to 21 days. There was no significant difference among the groups at day 4. At day 7, BMP2Pr-gNP group had the highest calcium content. At day 14, the groups with BMP2Pr-gNP and BMP2Pe-gNP had significantly higher calcium contents than OM group (indicated by one star in Figure 8). For example, at day 14 the calcium content of BMP2Pr, BMP2Pe-gNP and BMP2Pr-gNP groups was 18.1±0.3, 20.4±1.8, and 20.8±1.6 mg/dL, respectively, while that of OM group was 13.9±0.2 mg/dL. The calcium content of the NP groups at day 14 was slightly higher than that of BMP2Pr but the difference was not statistically significant. All osteogenic groups ultimately showed similar levels of mineralization after 21 days.

4. Discussion

The complex action of BMP2 is initiated on the cell surface by the interaction of the protein with type I and type II BMP2 receptors (BRI and BRII) (Caestecker, 2004; Sieber et al., 2009). There are pre-formed BMP2 receptor clusters on the cell surface that activate the Smad pathway (Attisano et al., 2001; Grunsven et al., 2005). BMP2 can also induce the complexation of those receptors present on detergent-resistant lipid membrane regions, most notably the Cholesterol-enriched and caveolae domains (Ross *et al.*, 2008; Sieber *et al.*, 2009). The BMP2 induced complexes can activate the Smad pathway and Smad-independent p38 pathway as well as internalization of the receptors (Cao *et al.*, 2005; Sieber *et al.*, 2009; Jimi *et al.*, 2010).

The expression of Dlx5 and Runx2 is the early event in the BMP2 signaling cascade. Dlx5 regulates the activity of the osteogenic master transcription factor Runx2 by Smad-dependent pathways which in turn, drives the expression of key osteogenic genes like OP and OC (Centrella *et al.*, 2004; Bae *et al.*, 2006). This may explain the observation that the expression of Dlx5 and Runx2 precedes that of OP and OC. When cultured in osteogenic medium, BMS cells eventually differentiate into bone-like cells with or without BMP2 supplementation as evident by cell morphology and immunostaining of osteogenic and vasculogenic markers. It is well established that cells aggregate and form clusters as they undergo osteogenic differentiation. For example, Facer and collaborators demonstrated that a 3D microenvironment created by a rotary cell culture system enhanced aggregation and osteogenic differentiation of marrow stromal progenitor cells (Facer et al., 2005). In another study, Yang and collaborators observed polymorphic cell aggregation near the invading capillaries and osteogenic differentiation within the cell aggregates when porous calcium phosphate scaffolds were implanted in the muscular tissue of dogs (Yang et al., 1997). Rai and collaborators observed a decreased cell number, increased cell aggregation, and enhanced osteogenic differentiation of pre-osteoblasts seeded in polycaprolactone scaffolds after 21 days (Rai et al., 2004).

In our study, supplement of free BMP2 protein to the osteogenic medium led to an increased expression of Dlx5 and Runx2 at early time points. This may be due to several factors. First, the half-life of BMP2 is short (7–16 minutes (Jones et al., 2006)). Therefore, transformations on the cell surface such as ligand diffusion, localization in distinct membrane domains, ligand-receptor binding, oligomerization and cluster formation, and receptor internalization might be the rate limiting steps in the cascade of osteogenic differentiation. Second, BMP2

protein is a potent inducer of osteogenic differentiation with a high binding affinity to the receptors. However, Runx2 protein overexpression regulates *Runx2* gene transcription by a negative feedback loop (Drissi et al., 2000). Therefore, *Runx2* and *Dlx5* are quickly down regulated after 7 days. These results are consistent with the findings of Lee (Lee et al., 2000) which show a reduction in the expression of *BMP2* mRNA after an immediate increase. The BMP peptide groups (grafted and free) showed an increase in gene expression at 14 days. Although the peptide itself has been shown to have affinities for both BRI and BRII in C3H10T1/2 cells (Saito *et al*., 2003), its binding affinities may differ from those of BMP2 protein. Therefore, it is possible that the interaction of the BMP peptide with BRI (and consequently, heterodimer formation) is kinetically slower than the BMP2 protein. Besides the difference in the receptor binding affinity, the stability of BMP2 peptide and protein may also differ. These effects may contribute to the delayed expression of Runx2 and Dlx5 in the peptide treated cells.

The expression pattern of Runx2 and Dlx5 does not exactly match the expression pattern of osteogenic markers in our experimental groups. It is possible that the sampling time points may not be ideal. It may also be due to the complexity of BMP signaling pathway. It has been demonstrated that an increase in the mRNA expression levels of *Dlx5* and *Runx2* alone is not sufficient for immediate induction of osteogenic markers (Lee *et al*., 2003). These results indicate that BMP2Pr and BMP2Pe grafted to NPs are longer-lasting and more effective in presenting proteins or peptides to cell surface receptors. The fluorescent images in Figure 2 and NP uptakes in Figure 3a demonstrate that a significant fraction of the NPs adhere to the surface of the BMS cells 24 h after incubation in osteogenic media. Therefore, NP grafting may increase the residence time of BMP2Pr and BMP2Pe. The NPs with 240 nm average diameter possess a relatively large surface area (25 m^2/g NPs) and potentially >7000 BMP2 molecules (7 nm × 3.5 nm (Laub et al., 2001)) can be grafted to a single NP. The large number of BMP2Pe or BMP2Pr per NP represents a multivalent form of the ligand for a stronger interaction with cell surface receptors, which are disposed in clusters on the cell surface (Rossi et al., 2003). For example, it has been demonstrated that BMP type II receptor forms 50–75 nm clusters on the cell surface and on clathrin-coated vesicles prior to receptor internalization and activation of p38 pathway (Hartung et al., 2006). Figure 9 shows schematically the effect of NP grafting on the presentation of BMP2 peptide/protein to cell surface receptors. A grafted NP provides a relatively high local concentration of the peptide/protein on the cell surface for interaction with a cluster of BRI/BRII receptors, thus forming BRI/BRII complexes. The formation of multiple localized BRI/BRII complexes could potentially lead to an intense activation of downstream osteogenic pathways.

PECAM is a cell-cell adhesion molecule implicated in lumen formation, cell polarity and vascular permeability in early angioblasts (Risau *et al*., 1995). The much higher expression of PECAM in BMP2Pe-gNP and BMP2Pr-gNP groups may be related to the expression of OP. We have shown previously that BMS cells seeded on aligned type I collagen tubes and cultured in osteogenic media, undergo simultaneous differentiation into osteogenic and vasculogenic lineages and produce a mineralized matrix (Henderson *et al*., 2008). Those results have revealed that OP expression level of the BMS cells cultured on collagen tubes are 5-fold higher than those cultured on tissue culture plates (Henderson *et al*., 2008).

Another study shows that FGF-2 triggers OP overexpression and vasculogenesis in murine aortic endothelial (MAE) cells (Leali et al., 2003). Furthermore, Hamada and collaborators have demonstrated that the OP-derived peptide SVVYGLR has as potent activity for tube formation in endothelial cells seeded in collagen gels as VEGF (Hamada et al., 2007).

Our findings demonstrate that the two NP grafted BMP2 groups (BMP2Pe-gNP and BMP2Pr-gNP) present higher activity toward osteogenic differentiation of BMS cells. NP grafting can potentially prevent the diffusion of protein or peptide away from the regeneration site, thus reducing the risks of bone overgrowth and tumor formation. Furthermore, the less costly BMP2 peptide with potentially lower side effects could be used as an alternative to BMP2 protein therapy in spine fusion and segmental fractures.

5. Conclusions

Osteogenic activity of the peptide LYLTSIASLETPVSSAKPIK, corresponding to residues 73–92 of the knuckle epitope of BMP2, grafted to self-assembled PLAF/PLEOF NPs was compared with that of BMP2 protein in bone marrow stromal (BMS) cells. The average size and breadth of the PLAF NPs was 240±80 nm. The extent of mineralization in BMS cells cultured with BMP2Pe grafted NPs was slightly higher than those cultured with BMP2Pe or BMP2 protein after 14 days of incubation, but all osteogenic groups reached similar levels of mineralization after 21 days. The expression level of OP, OC, and PECAM-1 in BMS cells cultured with BMP2Pe and BMP2Pr grafted NPs was significantly higher than those cultured with BMP2Pe or BMP2Pr (without grafting) after 21 days of incubation. The higher OP, OC, Runx2 and Dlx5 expressions in the NP grafted groups could be related to a more effective presentation of the peptide/protein to cell surface receptors, thus leading to a stronger interaction of the peptide/protein with clustered cell surface receptors. It can be argued that BMP2Pe or BMP2Pr grafted to NPs display much higher apparent affinity to cell surface receptors than the free BMP2Pe or BMP2Pr, leading to a more intense activation of osteogenic signaling pathways.

Acknowledgments

This work was supported by research grants to E. Jabbari from the National Science Foundation under grant Nos. CBET0756394, CBET0931998, and DMR1049381, the National Institutes of Health under Grant No. DE19180, and the Arbeitsgemeinschaft Fur Osteosynthesefragen (AO) Foundation under Grant No. C10-44J. The authors would like to thank Mr. Ryan Cassaro and Ms. Sowjanya Kadali for their assistance in the synthesis of cysteine-terminated BMP2Pe. The authors also thank Dr. Erin L. Connolly and Dr. Zhihuan Gao (Department of Biological Sciences at USC) for the use and assistance with RT-qPCR machine. The authors thank Dr. Jay Blanchette (Chemical Engineering at USC) for the use and assistance with Nikon inverted fluorescent microscope.

All sources of research support are identified in the acknowledgement section of the manuscript.

References

[1]. Attisano L, Silvestri C, Izzi L, et al. The transcriptional role of Smads nd FAST (FoxH1) in TGFb and activin signalling. Mol Cell Endocrinol. 2001; 180:3–11. [PubMed: 11451566]

[2]. Aubin JE, Liu F, Malaval L, et al. Osteoblast and chondroblast differentiation. Bone. 1995; 17:77S–83S. [PubMed: 8579903]

[3]. Bae SC, Lee YH. Phosphorylation, acetylation and ubiquitination: The molecular basis of RUNX regulation. Gene. 2006; 366:58–66. [PubMed: 16325352]

[4]. Behnam K, Phillips ML, Silva JD, et al. BMP binding peptide: a BMP-2 enhancing factor deduced from the sequence of native bovine bone morphogenetic protein/non-collagenous protein. J Orthop Res. 2005; 23:175–80. [PubMed: 15607890]

[5]. Caestecker MD. The transforming growth factor-b superfamily of receptors. Cytokine Growth Factor Rev. 2004; 15:1–11. [PubMed: 14746809]

[6]. Cao X, Chen D. The BMP signaling and in vivo bone formation. Gene. 2005; 357:1–8. [PubMed: 16125875]

[7]. Centrella M, Christakos S, McCarthy TL. Skeletal hormones and the C/EBP and Runx transcription factors: interactions that integrate and redefine gene expression. Gene. 2004; 342:13–24. [PubMed: 15527960]

[8]. Chen FM, Wu ZF, Sun HH, et al. Release of bioactive BMP from dextran-derived microspheres: A novel delivery concept. Int J Pharm. 2006; 307:23–32. [PubMed: 16260104]

[9]. Chen FM, Zhao YM, Sun HH, et al. Novel glycidyl methacrylated dextran (Dex-GMA)/gelatin hydrogel scaffolds containing microspheres loaded with bone morphogenetic proteins: Formulation and characteristics. J Contr Rel. 2007; 118:65–77.

[10]. Chung Y-I, Ahn K-M, Jeon S-H, et al. Enhanced bone regeneration with BMP-2 loaded functional nanoparticle–hydrogel complex. J Contr Rel. 2007; 121:91–99.

[11]. Ciarmela P, Wiater E, Smith SM, et al. Presence, actions, and regulation of myostatin in rat uterus and myometrial cells. Endocrinology. 2009; 150:906–914. [PubMed: 18845635]

[12]. Drissi H, Luc Q, Shakoori R, et al. Transcriptional autoregulation of the bone related CBFA1/RUNX2 gene. J Cell Physiol. 2000; 184:341–350. [PubMed: 10911365]

[13]. Facer SR, Zaharias RS, Andracki ME, et al. Rotary culture enhances pre-osteoblast aggregation and mineralization. J Dent Res. 2005; 84:542–7. [PubMed: 15914592]

[14]. Foster KA, Yazdanian M, Audus KL. Microparticulate uptake mechanisms of in-vitro cell culture models of the respiratory epithelium. J Pharm Pharmacol. 2001; 53:57–66. [PubMed: 11206193]

[15]. Fu YC, Nie H, Ho ML, et al. Optimized bone regeneration based on sustained release from three-dimensional fibrous PLGA/HAp composite scaffolds loaded with BMP-2. Biotechnol Bioeng. 2008; 99:996–1006. [PubMed: 17879301]

[16]. Gabet Y, Muller R, Regev E, et al. Osteogenic growth peptide modulates fracture callus structural and mechanical properties. Bone. 2004; 35:65–73. [PubMed: 15207742]

[17]. Grunsven LAV, Verstappen G, Huylebroeck D, et al. Smads and chromatin modulation. Cytokine Growth F R. 2005; 16:495–512.

[18]. Hamada Y, Egusa H, Kaneda Y, et al. Synthetic osteopontin-derived peptide SVVYGLR can induce neovascularization in artificial bone marrow scaffold biomaterials. Dent Mater J. 2007; 26:487–92. [PubMed: 17886451]

[19]. Hartung A, Bitton-Worms K, Rechtman MM, et al. Different routes of bone morphogenic protein (BMP) receptor endocytosis influence BMP signaling. Mol Cell Biol. 2006; 26:7791–805. [PubMed: 16923969]

[20]. Hassan MQ, Tare RS, Lee SH, et al. BMP2 Commitment to the osteogenic lineage involves activation of Runx2 by DLX3 and a homeodomain transcriptional network. J Biol Chem. 2006; 281:40515–40526. [PubMed: 17060321]

[21]. He X, Jabbari E. Material properties and cytocompatibility of injectable MMP degradable poly(lactide ethylene oxide fumarate) hydrogel as a carrier for marrow stromal cells. Biomacromolecules. 2007; 8:780–792. [PubMed: 17295540]

[22]. He X, Jabbari E. Synthesis and characterization of bioresorbable in situ crosslinkable ultra low molecular weight poly(lactide) macromer. J Mater Sci Mater Med. 2008; 19:311–318. [PubMed: 17597374]

[23]. He X, Ma J, Jabbari E. Effect of grafting RGD and BMP-2 protein-derived peptides to a hydrogel substrate on osteogenic differentiation of marrow stromal cells. Langmuir. 2008; 24:12508–12516. [PubMed: 18837524]

[24]. He X, Ma J, Jabbari E. Migration of marrow stromal cells in response to sustained release of stromal-derived factor-1alpha from poly(lactide ethylene oxide fumarate) hydrogels. Int J Pharm. 2010; 390:107–16. [PubMed: 20219655]

[25]. He X, Ma J, Mercado AE, et al. Cytotoxicity of paclitaxel in biodegradable self-assembled core-shell poly(lactide-co-glycolide ethylene oxide fumarate) nanoparticles. Pharm Res. 2008; 25:1552–1562. [PubMed: 18196205]

[26]. Henderson JA, He X, Jabbari E. Concurrent differentiation of marrow stromal cells to osteogenic and vasculogenic lineages. Macromol Biosci. 2008; 8:499–507. [PubMed: 17941111]

[27]. Hillger F, Herr G, Rudolph R, et al. Biophysical comparison of BMP-2, ProBMP-2, and the free pro-peptide reveals stabilization of the pro-peptide by the mature growth factor. J Biol Chem. 2005; 280:14974–14980. [PubMed: 15695507]

[28]. Hu Z, Peel SA, Ho SK, et al. Role of bovine bone morphogenetic proteins in bone matrix protein and osteoblast-related gene expression during rat bone marrow stromal cell differentiation. J Craniofac Surg. 2005; 16:1006–14. [PubMed: 16327548]

[29]. Huss R, Hoy CA, Deeg HJ. Contact- and growth factor-dependent survival in a canine marrow-derived stromal cell line. Blood. 1995; 85:2414–2421. [PubMed: 7537113]

[30]. Jabbari E, He X, Valarmathi M, et al. Material properties and bone marrow stromal cells response to in situ crosslinkable RGD-functionlized lactide-co-glycolide scaffolds. J Biomed Mater Res A. 2009; 89:124–137. [PubMed: 18431754]

[31]. Jimi E, Hirata S, Shin M, et al. Molecular mechanisms of BMP-induced bone formation: Cross-talk between BMP and NF-kB signaling pathways in osteoblastogenesis. Jpn Dent Sci Rev. 2010; 46:33–42.

[32]. Jones AL, Bucholz RW, Bosse MJ, et al. Recombinant human BMP-2 and allograft compared with autogenous bone graft for reconstruction of diaphyseal tibial fractures with cortical defects. A randomized, controlled trial. J Bone Joint Surg Am. 2006; 88:1431–41. [PubMed: 16818967]

[33]. Kaiser E, Colescott RL, Bossinger CD, et al. Color test for detection of free terminal amino groups in the solid-phase synthesis of peptides. Anal Biochem. 1970; 34:595–598. [PubMed: 5443684]

[34]. Kleeff J, Maruyama H, Ishiwata T, et al. Bone morphogenetic protein 2 exerts diverse effects on cell growth in vitro and is expressed in human pancreatic cancer in vivo. Gastroenterology. 1999; 116:1202–16. [PubMed: 10220513]

[35]. Langenfeld EM, Calvano SE, Abou-Nukta F, et al. The mature bone morphogenetic protein-2 is aberrantly expressed in non-small cell lung carcinomas and stimulates tumor growth of A549 cells. Carcinogenesis. 2003; 24:1445–54. [PubMed: 12819188]

[36]. Langenfeld EM, Langenfeld J. Bone Morphogenetic Protein-2 Stimulates Angiogenesis in Developing Tumors. Mol Cancer Res. 2004; 2:141–149. [PubMed: 15037653]

[37]. Laub M, Seul T, Schmachtenberg E, et al. Molecular modelling of bone morphogenetic protein-2 (BMP-2) by 3D-rapid prototyping. Materialwissenschaft und Werkstofftechnik. 2001; 32:926–930.

[38]. Leali D, Dell'Era P, Stabile H, et al. Osteopontin (Eta-1) and fibroblast growth factor-2 cross-talk in angiogenesis. J Immunol. 2003; 171:1085–93. [PubMed: 12847283]

[39]. Lee K-S, Kim H-J, Li Q-L, et al. Runx2 Is a common target of transforming growth factor beta-1 and bone morphogenetic protein 2, and cooperation between Runx2 and Smad5 induces osteoblast-specific gene expression in the pluripotent mesenchymal precursor cell line C2C12. Mol Cell Biol. 2000; 20:8783–8792. [PubMed: 11073979]

[40]. Lee M-H, Kim Y-J, Kim H-J, et al. BMP-2-induced Runx2 xxpression is mediated by Dlx5, and TGF-b opposes the BMP-2-induced osteoblast differentiation by suppression of Dlx5 expression. J Biol Chem. 2003; 278:34387–34394. [PubMed: 12815054]

[41]. Lee M-H, Kwon T-G, Park H-S, et al. BMP-2-induced Osterix expression is mediated by Dlx5 but is independent of Runx2. Biochem Biophys Res Commun. 2003; 309:689–694. [PubMed: 12963046]

[42]. Lee SH, Shin H. Matrices and scaffolds for delivery of bioactive molecules in bone and cartilage tissue engineering. Adv Drug Deliv Rev. 2007; 59:339–59. [PubMed: 17499384]

[43]. Lin H, Zhao Y, Sun W, et al. The effect of crosslinking heparin to demineralized bone matrix on mechanical strength and specific binding to human bone morphogenetic protein-2. Biomaterials. 2008; 29:1189–1197. [PubMed: 18083224]

[44]. Lisi S, Peterkova R, Peterka M, et al. Tooth morphogenesis and pattern of odontoblast differentiation. Connect Tissue Res. 2003; 44(Suppl 1):167–70. [PubMed: 12952192]

[45]. Liu HW, Chen CH, Tsai CL, et al. Targeted delivery system for juxtacrine signaling growth factor based on rhBMP-2-mediated carrier-protein conjugation. Bone. 2006; 39:825–36. [PubMed: 16782421]

[46]. Mauney JR, Blumberg J, Pirun M, et al. Osteogenic differentiation of human bone marrow stromal cells on partially demineralized bone scaffolds in vitro. Tissue Eng. 2004; 10:81–92. [PubMed: 15009933]

[47]. McKay B, Sandhu HS. Use of recombinant human bone morphogenetic protein-2 in spinal fusion applications. Spine. 2002; 27:S66–S85. [PubMed: 12205423]

[48]. Mercado AE, He XZ, Xu WJ, et al. The release characteristics of a model protein from self-assembled succinimide-terminated poly(lactide-co-glycolide ethylene oxide fumarate) nanoparticles. Nanotechnology. 2008; 19:325609. [PubMed: 21828822]

[49]. Mercado AE, Ma J, He X, et al. Release characteristics and osteogenic activity of recombinant human bone morphogenetic protein-2 grafted to novel self-assembled poly(lactide-co-glycolide fumarate) nanoparticles. J Contr Rel. 2009; 140:148–156.

[50]. Nadri S, Soleimani M, Hosseni RH, et al. An efficient method for isolation of murine bone marrow mesenchymal stem cells. Int J Dev Biol. 2007; 51:723–9. [PubMed: 17939119]

[51]. Owen TA, Aronow M, Shalhoub V, et al. Progressive development of the rat osteoblast phenotype in vitro: reciprocal relationships in expression of genes associated with osteoblast proliferation and differentiation during formation of the bone extracellular matrix. J Cell Physiol. 1990; 143:420–430. [PubMed: 1694181]

[52]. Perez VAD, Ali Z, Alastalo TP, et al. BMP promotes motility and represses growth of smooth muscle cells by activation of tandem Wnt pathways. J Cell Biol. 2011; 192:171–188. [PubMed: 21220513]

[53]. Pfaffl MW. A new mathematical model for relative quantification in real-time RT PCR. Nucleic Acids Res. 2001; 29:e45. [PubMed: 11328886]

[54]. Rai B, Teoh SH, Ho KH, et al. The effect of rhBMP-2 on canine osteoblasts seeded onto 3D bioactive polycaprolactone scaffolds. Biomaterials. 2004; 25:5499–506. [PubMed: 15142731]

[55]. Raida M, Clement JH, Leek RD, et al. Bone morphogenetic protein 2 (BMP-2) and induction of tumor angiogenesis. J Cancer Res Clin Oncol. 2005; 131:741–750. [PubMed: 16136355]

[56]. Redhead HM, Davis SS, Illum L. Drug delivery in poly(lactide-co-glycolide) nanoparticles surface modified with poloxamer 407 and poloxamine 908: in vitro characterisation and in vivo evaluation. J Contr Rel. 2001; 70:353–363.

[57]. Ripamonti U, Reddi AH. Tissue engineering, morphogenesis, and regeneration of the periodontal tissues by bone morphogenetic proteins. Crit Rev Oral Biol Med. 1997; 8:154–63. [PubMed: 9167090]

[58]. Risau W, Flamme l. Vasculogenesis. Annu. Rev. Cell Dev. Biol. 1995; 11:73–91. [PubMed: 8689573]

[59]. Ross S, Hill CS. How the Smads regulate transcription. Int J Biochem Cell B. 2008; 40:383–408.

[60]. Rossi EA, Sharkey RM, McBride W, et al. Development of new multivalent bispecific agents for pretargeting tumor localization and therapy. Clin Cancer Res. 2003; 9:3886S–96S. [PubMed: 14506187]

[61]. Sahoo SK, Panyam J, Prabha S, et al. Residual polyvinyl alcohol associated with poly (D,L-lactide-co-glycolide) nanoparticles affects their physical properties and cellular uptake. J Contr Rel. 2002; 82:105–114.

[62]. Saito A, Suzuki Y, Ogata S-i, et al. Activation of osteo-progenitor cells by a novel synthetic peptide derived from the bone morphogenetic protein-2 knuckle epitope. Biochim Biophys Acta. 2003; 1651:60–67. [PubMed: 14499589]

[63]. Saito A, Suzuki Y, Ogata S-I, et al. Prolonged ectopic calcification induced by BMP-2-derived synthetic peptide. J Biomed Mater Res A. 2004; 70:115–121. [PubMed: 15174115]

[64]. Shi X, Wang Y, Varshney RR, et al. Microsphere-based drug releasing scaffolds for inducing osteogenesis of human mesenchymal stem cells in vitro. Eur J Pharm Sci. 2010; 39:59–67. [PubMed: 19895885]

[65]. Shields LBE, Raque GH, Glassman SD, et al. Adverse effects associated with high-dose recombinant human bone morphogenetic protein-2 use in anterior cervical spine fusion. Spine. 2006; 31:542–547. [PubMed: 16508549]

[66]. Sieber C, Kopf J, Hiepen C, et al. Recent advances in BMP receptor signaling. Cytokine Growth F R. 2009; 20:343–355.

[67]. Vehof JWM, Ruijter AED, Spauwen PHM, et al. Influence of rhBMP-2 on rat bone marrow stromal cells cultured on titanium fiber mesh. Tissue Eng. 2001; 7:373–383. [PubMed: 11506727]

[68]. Wei G, Jin Q, Giannobile WV, et al. The enhancement of osteogenesis by nano-fibrous scaffolds incorporating rhBMP-7 nanospheres. Biomaterials. 2007; 28:2087–2096. [PubMed: 17239946]

[69]. Wozney JM. Overview of bone morphogenetic proteins. Spine. 2002; 27:S2–S8. [PubMed: 12205411]

[70]. Xie JW, Wang CH. Self-assembled biodegradable nanoparticles developed by direct dialysis for the delivery of paclitaxel. Pharm Res. 2005; 22:2079–2090. [PubMed: 16132339]

[71]. Yamagiwa H, Endo N, Tokunaga K, et al. In vivo bone-forming capacity of human bone marrow-derived stromal cells is stimulated by recombinant human bone morphogenetic protein-2. J Bone Miner Metab. 2001; 19:20–28. [PubMed: 11156469]

[72]. Yang HS, La W-G, Bhang SH, et al. Heparin-Conjugated Fibrin as an Injectable System for Sustained Delivery of Bone Morphogenetic Protein-2. Tissue Eng A. 2010; 16:1225–1233.

[73]. Yang ZJ, Yuan H, Zou P, et al. Osteogenic responses to extraskeletally implanted synthetic porous calcium phosphate ceramics: an early stage histomorphological study in dogs. J Mater Sci Mater Med. 1997; 8:697–701. [PubMed: 15348821]

[74]. Yasko AW, Lane JM, Fellinger EJ, et al. The healing of segmental bone defects, induced by recombinant human bone morphogenetic protein (rhBMP-2). J Bone Jt Surg Am. 1992; 74:659–670.

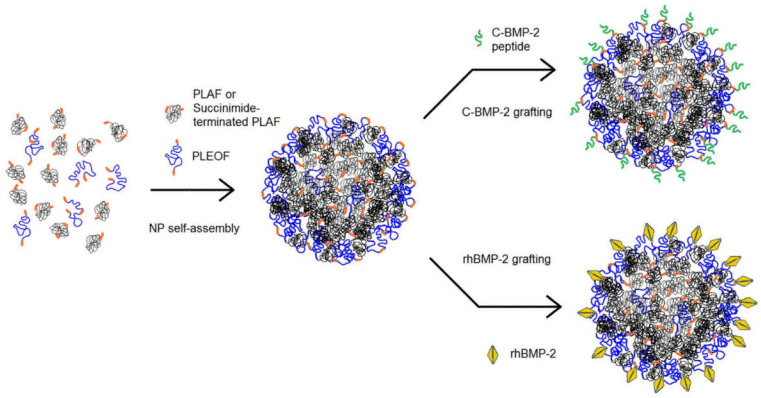

Figure 1.

Schematic diagram for the self-assembly of PLAF (or PLAF-NHS) and PLEOF blend to produce NPs and the grafting of cysteine-terminated BMP2Pe or BMP2Pr to the NPs.

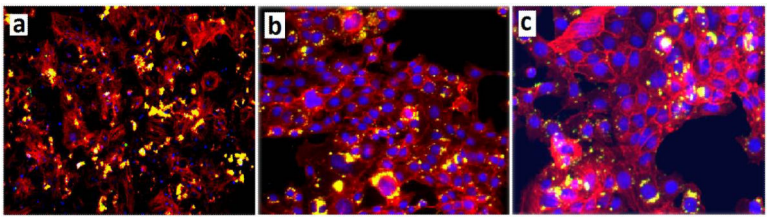

Figure 2.

Fluorescent images of FITC-loaded NPs without grafting (a), with BMP2 peptide grafting (b), and with BMP2 protein grafting (c) attached to BMS cells in osteogenic media. The cell nuclei and cytoskeleton were stained with DAPI (blue) and phalloidin (red), respectively (yellow in the images is the overlap of red FITC and red phalloidin).

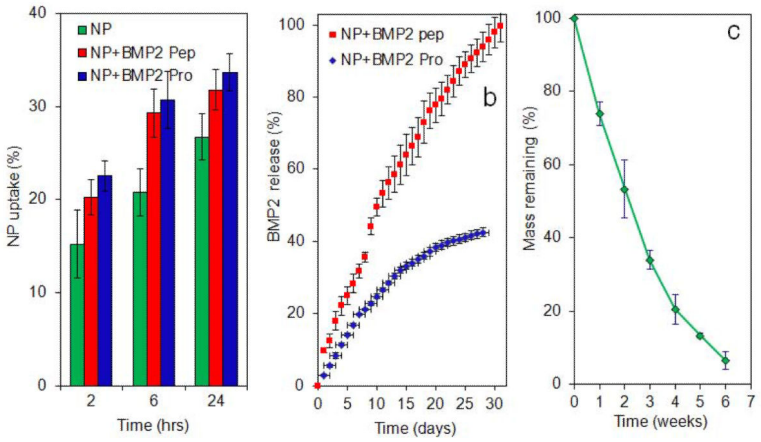

Figure 3.

(a) Effect of BMP2 peptide or BMP2 protein grafted NPs on uptake of FITC-loaded NPs with incubation time; (b) release kinetics of BMP2 peptide (red) and BMP2 protein (enzymatically active, blue) with incubation time; (c) degradation kinetics (mass loss) of the NPs with incubation time. The star in Figure 3a indicates statistically significant difference (s.d.; $p<0.05$) between the uptake of peptide/protein grafted NPs and ungrafted NPs for a given time point. Error bars correspond to means ± 1 SD for n = 3.

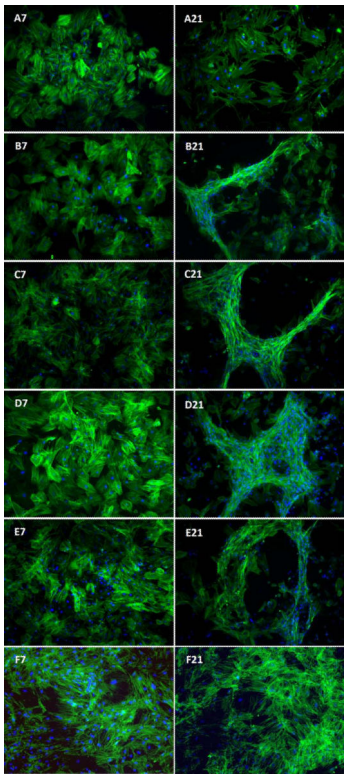

Figure 4.

Effect of supplementing culture media with BMP2Pe or BMP2Pr grafted NPs on morphology of the BMS cells after 7 and 21 days. The left and right fluorescent images are for 7 and 21 days, respectively. In the images, cell nuclei and actin filaments of the cytoskeleton are stained with DAPI (blue) and phalloidin (green), respectively. Groups include BMS cells cultured in basal media (A7 and A21), osteogenic media (OM; B7 and B21), OM supplemented with 200 ng/mL BMP2Pe (C7 and C21), OM supplemented with 200 ng/mL BMP2Pe grafted NPs (D7 and D21), OM supplemented with 200 ng/mL BMP2 protein (E7 and E21), and OM supplemented with 200 ng/mL BMP2Pr grafted NPs (F7 and F21).

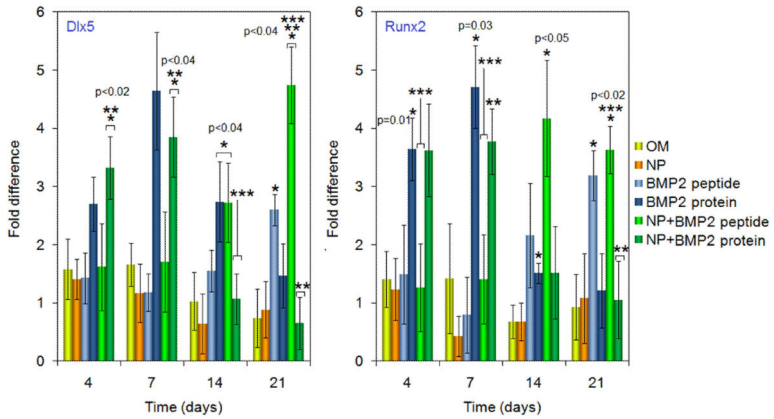

Figure 5.

Effect of supplementing culture media with BMP2Pe or BMP2Pr grafted NPs on mRNA expression level (as fold difference) of master transcription factors Dlx5 and Runx2. The expression level of S16 control gene was used as the reference and the fold difference in expression was normalized to that at time zero. Groups include BMS cells cultured in OM, OM supplemented with blank NPs, OM supplemented with BMP2 protein, OM supplemented with BMP2Pe, OM supplemented with BMP2Pe grafted NPs, and OM supplemented with BMP2Pr grafted NPs. One star indicates statistically significant difference (s. d.; $p<0.05$) between the test group and OM, two stars between the test group and free BMP2Pe, and three stars between the test group and BMP2Pr. Error bars correspond to means ± 1 SD for n = 3.

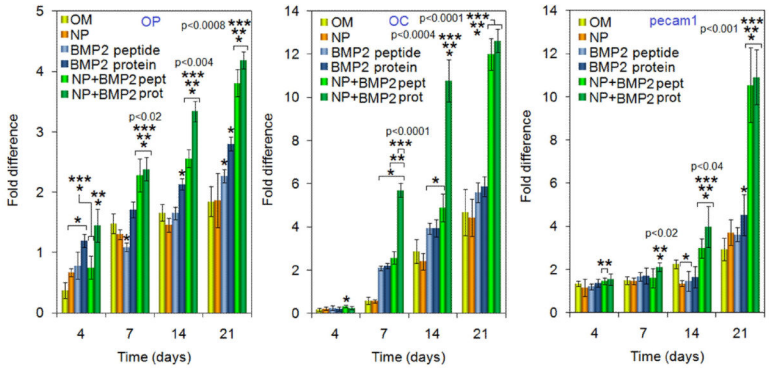

Figure 6.

Effect of supplementing culture media with BMP2Pe or BMP2Pr grafted NPs on mRNA expression level (as fold difference) of osteogenic markers OP and OC, and vasculogenic marker PECAM-1. The expression level of S16 control gene was used as the reference and the fold difference in expression was normalized to that at time zero. Groups include BMS cells cultured in OM, OM supplemented with blank NPs, OM supplemented with BMP2 protein, OM supplemented with BMP2Pe, OM supplemented with BMP2Pe grafted NPs, and OM supplemented with BMP2Pr grafted NPs. One star indicates statistically significant difference (s.d.; $p<0.05$) between the test group and OM, two stars between the test group and free BMP2Pe, and three stars between the test group and BMP2Pr. Error bars correspond to means ± 1 SD for n = 3.

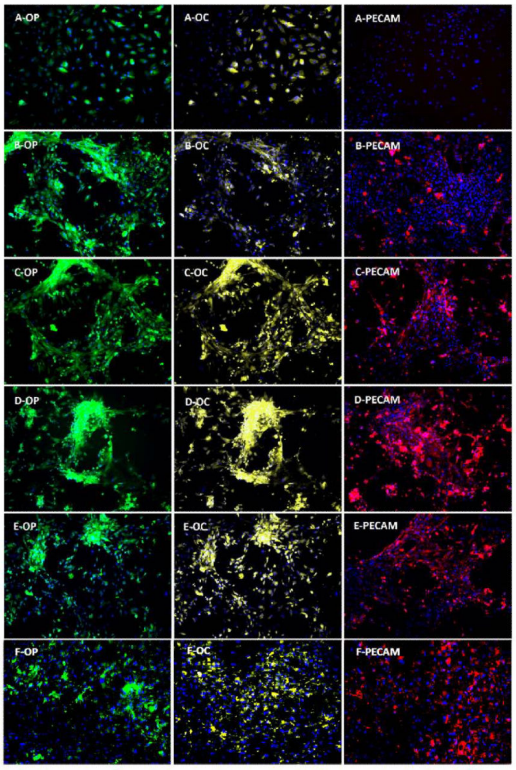

Figure 7.

Effect of supplementing culture media with BMP2Pe or BMP2Pr grafted NPs on the expression of osteogenic (OP and OC) and vasculogenic (PECAM-1) markers. Fluorescent images on the left, center, and right show expression of OP (green), OC (light yellow), and PECAM (red), respectively. Groups include BMS cells cultured in basal media (A-OP, A-OC, A-PECAM), OM (B-OP, B-OC, B-PECAM), OM supplemented with BMP2Pe (C-OP, C-OC, C-PECAM), OM supplemented with BMP2Pe grafted NPs (D-OP, D-OC, D-PECAM), OM supplemented with BMP2 protein (E-OP, E-OC, E-PECAM), and OM supplemented with BMP2Pr grafted NPs (F-OP, F-OC, F-PECAM).

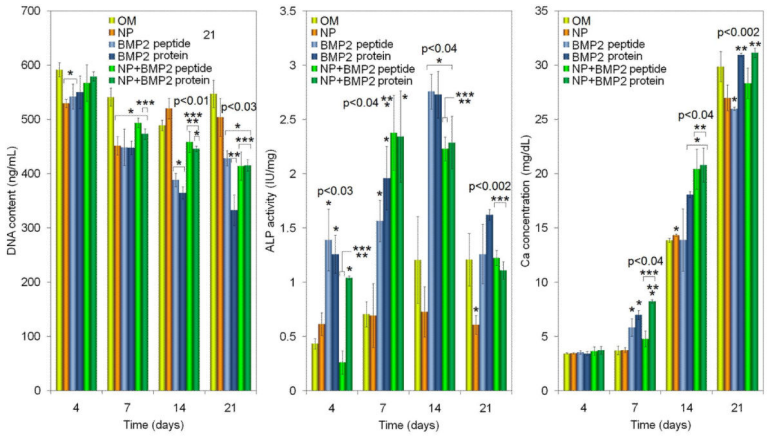

Figure 8.

Effect of supplementing culture media with BMP2Pe or BMP2Pr grafted NPs on BMS cell count (DNA), ALPase activity, and calcium content with incubation time. Groups include BMS cells cultured in OM, OM supplemented with blank NPs, OM supplemented with BMP2 protein, OM supplemented with BMP2Pe, OM supplemented with BMP2Pe grafted NPs, and OM supplemented with BMP2Pr grafted NPs. One star indicates statistically significant difference (s.d.; $p<0.05$) between the test group and OM, two stars between the test group and free BMP2Pe, and three stars between the test group and BMP2Pr. Error bars correspond to means ± 1 SD for n = 3.

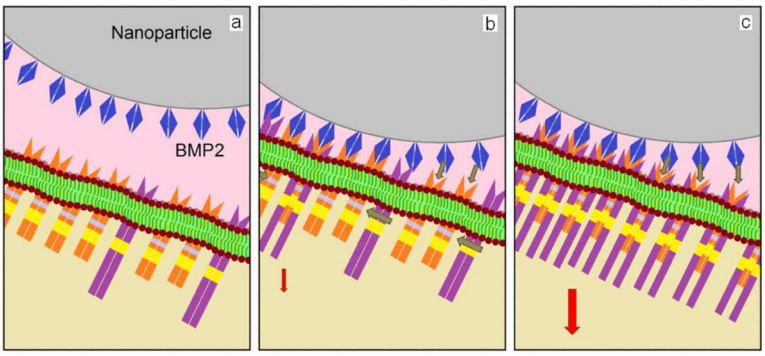

Figure 9.

Schematic diagram showing the presentation of NP grafted BMP2 peptides/proteins to cell surface receptors: (a) an NP (gray) grafted with many BMP2 peptides/proteins (blue) provides a high concentration of the peptide/protein locally on the cell surface for interaction with a cluster of BRI (orange/yellow) and BRII (violet/yellow) receptors; many BMP2 peptides/proteins on the NP interact locally with BRI and BRII receptors (b) to form BRI/BRII complexes (c); the formation of multiple localized BRI/BRII complexes leads to an intense activation of downstream osteogenic pathways (shown by red arrow).